

Original article

Phase transformation behaviors and mechanical properties of NiTi endodontic files after gold heat treatment and blue heat treatmentXiao-Mei Hou¹⁾, Yin-Jie Yang²⁾, and Jun Qian¹⁾¹⁾The Second Dental Center of Peking University School of Stomatology, Beijing, P. R. China²⁾Department of Stomatology, Beijing Xicheng District Xinjiekou Community Health Service Center, Beijing, P. R. China

(Received August 16, 2019; Accepted February 6, 2020)

Abstract: WaveOne Gold, ProTaper Gold, Reciproc Blue, ProTaper Next, WaveOne and ProTaper files were selected to compare the phase transformation behaviors and mechanical properties of nickel-titanium (NiTi) rotary files after gold heat and blue heat treatments. The reverse transformation finishing point temperatures of WaveOne Gold, ProTaper Gold, ProTaper Next and WaveOne were higher than those of the other two instruments investigated. At a deflection of 0.5 mm, the loads were significantly varied except for ProTaper Next and ProTaper Gold. At a deflection of 3.0 mm, the loads of Reciproc Blue and WaveOne Gold were significantly varied compared to WaveOne and ProTaper. Cycles to failure were reduced in the order of WaveOne Gold, Reciproc Blue, ProTaper Gold, ProTaper Next, WaveOne and ProTaper. NiTi instruments after gold heat and blue heat treatments exhibited significantly higher bending properties and cyclic fatigue resistances, representing an improved performance over traditional and M-wire instruments.

Keywords; blue heat treatment, gold heat treatment, nickel-titanium, phase transformation, rotary instrument

Introduction

Preparation of root canals requires cleaning and molding of the space in the root canal without creating errors such as ledges, zips, or perforations [1,2]. Root canal instruments made of nickel-titanium (NiTi) alloy have been employed for this purpose for 30 years [3,4]. These NiTi rotary instruments have been widely applied in endodontics due to their unique properties resulting from the austenite-martensite transition, including super-elasticity, great flexibility, and shape-memory effects [5-7]. However, torsional forces and cyclic fatigue may result in unanticipated fracture of NiTi rotary instruments within the root canal [8,9].

To date, various methods have been used to prevent fractures of NiTi rotary files and to improve their effectiveness, safety and reliability. The properties of endodontic instruments can be selected by identifying suitable material microstructures and processing technologies. Currently, new alloys possessing superior mechanical properties are used by manufacturers [10-13]. Raw alloy metals with highly preferred microstructures and material properties are chosen or custom designed for the manufacture of NiTi files, and great efforts have been made to fabricate new instruments over the last few decades [14,15]. Varied fabrication processes that optimize phase transformation behaviors and mechanical properties are employed for production of these improved instruments [16].

To create suitable microstructures and optimize the phase transformation behaviors of NiTi alloys, thermal treatments have been performed, resulting in products such as R-phase wire, M-wire, and controlled memory wire (CM-wire). The mechanical properties and reliability of NiTi files have thus been improved. Recently, NiTi files of WaveOne Gold (Dentsply Maillefer, Ballaigues, Switzerland), ProTaper Gold (Dentsply, Tulsa Dental Specialties, Tulsa, OK, USA) and Reciproc Blue (VDW,

Munich, Germany) were introduced as new instruments resulting from modern thermal treatment procedures. Among them, WaveOne Gold is the new version of the well-known WaveOne file. The dimension and cross-sectional shape of WaveOne Gold have been optimized, while its reciprocation motion has been preserved. The design is a parallelogram cross-section with two cutting edges. In addition, the off-center design that is used in previous ProTaper Next files (Dentsply Maillefer, Ballaigues, Switzerland), is also used in WaveOne Gold files. Gold heat treatment for WaveOne Gold is carried out after production by heating and slow cooling of the files, differing from M-wire technology [17]. The flexibility of WaveOne Gold files is thus increased. Metallurgically, gold heat treated files are more varied, providing higher flexibility than traditional NiTi files and M-wire files [17].

Using proprietary advanced metallurgy, ProTaper Gold instruments have also been developed. The geometry of ProTaper Gold is identical to that of ProTaper Universal files (Dentsply Maillefer) in having a convex triangular cross-section, and the progressively tapered design enhances both safety and cutting efficiency. Thus far, ProTaper Gold has been developed using advanced metallurgy methods involving heat treatment [7,18]. The manufacturer claims that these instruments have fatigue resistance superior to that of ProTaper Universal.

Reciproc Blue, the newest version of Reciproc, has an S-shaped cross-section, containing two cutting edges and a non-cutting tip [19]. Its manufacture involves a new form of heat treatment creating varied molecular structures and a unique blue oxide surface layer. Recently, it has been reported that Reciproc Blue shows improved all-around performance compared to that of conventional M-Wire Reciproc, demonstrating higher flexibility, fatigue resistance and reduced microhardness, while maintaining similar surface characteristics [20]. Silva et al. have further reported that Reciproc Blue has an increased angle of rotation to fracture but a lower torque to failure than those of the original Reciproc [21].

Currently, there is a need for clinicians to understand the features of different files to best meet the anatomic challenges of root canals. However, the effects of new fabrication processes on the mechanical properties of these files (WaveOne Gold, ProTaper Gold, and Reciproc Blue) may be misleading if information on their phase transformation behaviors is unclear. The mechanical properties of NiTi instruments vary greatly with phase transformation behaviors and are easily changed by chemical composition, heat treatment and manufacturing processes. Therefore, the aim of the present study was to investigate the thermal behaviors, bending properties and cyclic fatigue resistance of these three new files in comparison with three control files (ProTaper Next, WaveOne and ProTaper). The null hypothesis was that there would be no differences in phase transformation behavior, bending resistance or cyclic fatigue resistance among these instruments.

Materials and Methods**NiTi files**

The following rotary NiTi instruments were used in this study: WaveOne Gold (Primary, 25 mm), ProTaper Gold (F2, 25 mm), Reciproc Blue (R25, 25 mm), ProTaper Next (X2, 25 mm), WaveOne (Primary, 25 mm) and ProTaper (F2, 25 mm).

Instrument Geometry

At the D7 level, the cross-sectional geometries of the instruments were

Correspondence to Dr. Jun Qian, The Second Dental Center of Peking University School of Stomatology, No. 66 Anli Road, Chaoyang District, Beijing 100101, P. R. China
E-mail: atlasatlas@163.com

J-STAGE Advance Publication: December 7, 2020

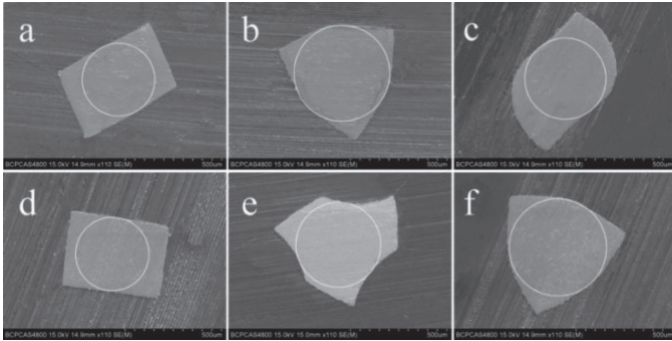
Color figures can be viewed in the online issue at J-STAGE.

doi.org/10.2334/josnusd.19-0331

DN/JST.JSTAGE/josnusd/19-0331

Table 1 Endodontic motor and program specifications for the file types investigated

Files	Handpiece	Electric motor	Speed /rpm	Torque/N cm
WaveOne Gold	6:1	SILVER RECOPROC, VDW, Germany	350	-
ProTaper Gold	20:1	ENDO-MATE DT, NSK, Japan	300	5.5
Reciproc Blue	6:1	SILVER RECOPROC, VDW, Germany	300	-
ProTaper Next	20:1	ENDO-MATE DT, NSK, Japan	300	5.5
WaveOne	6:1	SILVER RECOPROC, VDW, Germany	350	-
ProTaper	20:1	ENDO-MATE DT, NSK, Japan	300	5.5

**Fig. 1** Cross-sectional configurations for the six files at the maximum stress point (110 \times). a, b, c, d, e, and f represent WaveOne Gold, ProTaper Gold, Reciproc Blue, ProTaper Next, WaveOne, and ProTaper, respectively.

investigated using scanning electron microscopy (SEM). The area of the D7 level was measured using commercially available software, ImageJ 2x (National Institutes of Health, San Jose, CA, USA).

Differential scanning calorimetry

Differential scanning calorimetry (DSC, 200F3, Netzsch, Germany) analysis was performed with the specimens under argon gas. The temperature was increased from room temperature to 100°C, followed by a decrease to -100°C and ultimately increased back to 100°C. The heating and cooling rates were 10°C/min. The specimens were chosen from blade portions of the files. The average weight and length of the specimens were 20 ± 1 mg and 2-3 mm. The martensitic transformation-starting and finishing points (Ms, Mf), as well as the reverse transformation-starting and finishing points (As, Af) were determined according to a previous study [22]. Furthermore, individual or combined peak areas (enthalpies) were also calculated from the DSC curves.

Bending resistance test

The bending resistance test was performed using a biomechanical testing machine (ElectroForce 3100 Bose, TA instruments, New Castle, DE, USA) at a room temperature of 25°C. After the handles had been removed, each specimen was clamped at 9.5 mm, as measured from the tip. The loading point was located at 3.0 mm from the tip. At loading and unloading speeds of 1.0 mm/min, the deflection reached 4.0 mm before the unloading step was initiated. Finally, the force was reduced to 0 N.

Cyclic fatigue test

The static cyclic fatigue testing device consisted of a main frame and a stainless steel block containing an artificial canal with a curvature of 60° and radius of 3.5 mm. The curvature center of the canal was located at 7 mm from the tip of the instrument. The instruments were rotated at speeds recommended by the manufacturers using different reduction handpieces that were powered by torque-controlled electric motors (Table 1). Lubricant (Vaseline, Tianjin, P. R. China) was applied to reduce the friction between the files and the artificial canal walls. All instruments were loaded until fracture. Time to fracture was recorded using a chronometer and the number of cycles to failure (NCF) for each instrument calculated by multiplying the fracture time by the number of rotations per second. The length of the fractured tip was also measured. The fracture surface of the files was observed using SEM.

Table 2 Cross-sectional area and inner core area (mm²) for the six files at the maximum stress point

	Cross-sectional area	Inner core area
WaveOne Gold	0.21	0.12
ProTaper Gold	0.25	0.20
Reciproc Blue	0.25	0.14
ProTaper Next	0.21	0.12
WaveOne	0.23	0.15
ProTaper	0.27	0.21

Statistical analyses

All data are generally presented as the mean \pm standard deviation. Statistical analysis was performed using SPSS 21.0 software (SPSS Inc, Chicago, IL, USA). The normality of the data was analyzed using the Kolmogorov-Smirnov test. Abnormally distributed data were also presented as the median with interquartile range (IQR). The homogeneity of variables was analyzed using the Levene test. For normally distributed data with homoscedasticity, comparisons among groups were performed using one-way analysis of variance with the Tukey *post hoc* test. Otherwise, comparisons were performed using the Kruskal-Wallis H test with a Bonferroni *post hoc* test. Differences at $P < 0.05$ were considered statistically significant.

Results

Instrument geometry

Cross-sectional shapes of the six examined files at the maximum stress points (D7) during the cyclic fatigue resistance test were investigated using SEM. Images shown in Fig. 1 demonstrate the differences in cross-sectional shapes observed by SEM. WaveOne Gold (Fig. 1a) and ProTaper Next (Fig. 1d) had small inner core areas of approximately 0.12 mm², as indicated by the white circles, while ProTaper Gold (Fig. 1b) and ProTaper (Fig. 1f) had large inner core areas (0.20-0.21 mm²) (Table 2).

Differential scanning calorimetry

The DSC heating and cooling cycles of the six NiTi files are shown in Fig. 2. During heating, two prominent endothermic peaks were observed in the curves of the three new instruments tested—WaveOne Gold, ProTaper Gold and Reciproc Blue—similar to the conventional ProTaper files. Single endothermic peaks were observed in the ProTaper Next and WaveOne files. As shown in Table 3, all data except ΔH of Cooling in the Waveone group and ΔH of Heating in the ProTaper group were normally distributed, and the Mf data for cooling showed no homoscedasticity ($P = 0.022$). All parameters differed significantly among the six groups (all $P \leq 0.01$). The Af temperatures, those at which the transformation of austenitic NiTi upon heating ceased, exceeded 50°C for WaveOne Gold (51.6), ProTaper Gold (50.6), ProTaper Next (51.4) and WaveOne (53.0). In contrast, the Af temperatures of Reciproc Blue and ProTaper were 38.4 and 20.7°C, respectively. During the cooling process, single peaks were observed except for the Reciproc Blue sample, suggesting phase transformation from austenite to martensite. The Mf temperatures, indicating the appearance of martensite NiTi during cooling, were found to be about 20°C for WaveOne Gold (22.0), ProTaper Gold (16.0), ProTaper Next (21.5) and WaveOne (17.9) (Table 3). Mf temperatures for Reciproc Blue (-83.3) and ProTaper (-11.6) were also significantly lower than those of the aforementioned four files.

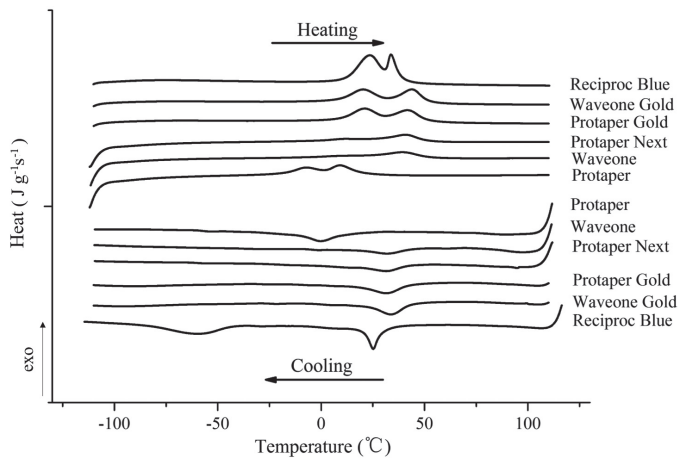


Fig. 2 DSC cooling and heating curves of the six files investigated

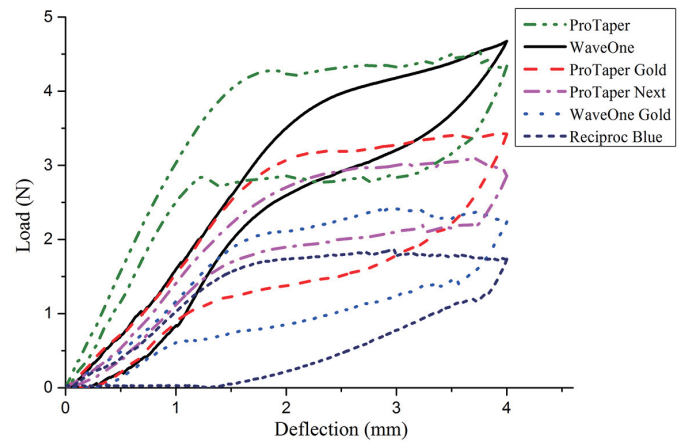


Fig. 3 Load-deflection curves for the six files

Table 3 Phase transformation temperatures (°C) and ΔH (J/g) measured for the files studied

		WaveOne Gold	ProTaper Gold	Reciprocal Blue	ProTaper Next	WaveOne	ProTaper	F/H	P	
Cooling	Ms (mean \pm SD)	43.8 \pm 0.3 ^{def}	43.0 \pm 0.8 ^{def}	20.37 \pm 0.5 ^{abdef}	45.1 \pm 1.1 ^{abcf}	44.4 \pm 1.0 ^{bef}	13.8 \pm 0.9 ^{abede}	1555.63	<0.001	
	Mf (mean \pm SD)	22.0 \pm 0.7 ^f	16.1 \pm 4.9 ^{acdf}	-83.3 \pm 0.7 ^{ad}	21.5 \pm 7.1 ^{bef}	17.9 \pm 3.5 ^{ef}	-11.6 \pm 3.3 ^a	22.93	<0.001	
	ΔH (mean \pm SD)	5.6 \pm 0.3	5.2 \pm 0.4	10.5 \pm 0.6 ^e	3.8 \pm 1.8	2.0 \pm 0.5 ^e	3.7 \pm 1.8		21.567	0.001
	ΔH (median, IQR)	5.5 (0.3)								
Heating	As (mean \pm SD)	8.5 \pm 0.4 ^{bdef}	6.5 \pm 1.9 ^{acdef}	12.0 \pm 0.5 ^{abdef}	0.2 \pm 1.2 ^{abcef}	-3.9 \pm 0.8 ^{abdef}	-18.2 \pm 0.4 ^{abede}	573.79	<0.001	
	Af (mean \pm SD)	51.6 \pm 0.6 ^{bcef}	50.6 \pm 0.7 ^{bcef}	38.4 \pm 0.6 ^{abdef}	51.4 \pm 0.3 ^{bcef}	53.00 \pm 0.4 ^{abdef}	20.7 \pm 0.4 ^{abede}	3007.18	<0.001	
	ΔH (mean \pm SD)	10.7 \pm 0.2	10.8 \pm 0.7	15.3 \pm 0.3 ^{de}	3.3 \pm 0.2 ^c	3.2 \pm 0.3 ^c	6.1 \pm 0.5	26.687	<0.001	
	ΔH (median, IQR)						6.0 (0.63)			

All data are generally presented as mean \pm standard deviation (SD). The normality of data was analyzed using the Kolmogorov-Smirnov test. Abnormally distributed data are also presented as median (IQR). The homogeneity of variables was analyzed using the Levene test. Comparisons among normally distributed data with homoscedasticity were performed using ANOVA with Tukey *post hoc* analysis. Otherwise, the Kruskal-Wallis H test with Bonferroni *post hoc* test was performed. *n* = 5 in each group. ^aCompared with WaveOne Gold (*P* < 0.05). ^bCompared with ProTaper Gold (*P* < 0.05). ^cCompared with Reciprocal Blue (*P* < 0.05). ^dCompared with ProTaper Next (*P* < 0.05). ^eCompared with WaveOne (*P* < 0.05). ^fCompared with ProTaper (*P* < 0.05).

Table 4 Loads at deflections of 0.5 and 3.0 mm for the six files

		WaveOne Gold	ProTaper Gold	Reciprocal Blue	ProTaper Next	WaveOne	ProTaper	H	P
Load at 0.5 mm	Mean \pm SD	0.41 \pm 0.07 ^{ef}	0.53 \pm 0.13 ^f	0.32 \pm 0.09 ^{ef}	0.52 \pm 0.06 ^f	0.77 \pm 0.07 ^{bc}	1.42 \pm 0.34 ^{abcd}	39.042	<0.001
	Median (IQR)					4.33 (0.23)	4.15 (0.33)	42.809	<0.001
Load at 3.0 mm	Mean \pm SD	2.34 \pm 0.17 ^{ef}	3.12 \pm 0.18	2.09 \pm 0.18 ^{ef}	3.10 \pm 0.25	4.39 \pm 0.25 ^{bc}	4.23 \pm 0.48 ^{bc}		
	Median (IQR)					4.33 (0.23)	4.15 (0.33)		

All data are generally presented as mean \pm standard deviation (SD). The normality of data was analyzed using the Kolmogorov-Smirnov test. Abnormally distributed data are also presented as median (IQR). The homogeneity of variables was analyzed using the Levene test. Comparisons among groups were performed using the Kruskal-Wallis H test with Bonferroni *post hoc* test. *n* = 8 in each group. ^aCompared with WaveOne Gold (*P* < 0.05). ^bCompared with ProTaper Gold (*P* < 0.05). ^cCompared with Reciprocal Blue (*P* < 0.05). ^dCompared with ProTaper Next (*P* < 0.05). ^eCompared with WaveOne (*P* < 0.05). ^fCompared with ProTaper (*P* < 0.05).

Bending resistance test

The plots in Fig. 3 show the relay load versus deflection of the six instruments during flexural tests. The loads of all six files increased almost linearly initially, indicative of their elastic deformations. Subsequently, plateaus that represented the stress-induced phase transformation were reached. During the unloading procedures, five instruments (WaveOne Gold, ProTaper Gold, ProTaper Next, WaveOne, and ProTaper) achieved these plateaus smoothly in the load-deflection curves, indicating the reverse transformation. Finally, the elastic recoveries were noted, generating small residual deflections, except for Reciprocal Blue, which formed an evident residual deflection. The plateau of WaveOne was steeper than for the other files.

The loads of the six NiTi files at deflections of 0.5 and 3 mm are listed in Table 4. Data at 3.0 mm in the WaveOne and ProTaper groups were abnormally distributed and data at 0.5 mm showed no homoscedasticity (*P* = 0.002). The loads data at two deflections differed significantly among the six files (*P* < 0.001). The load for Reciprocal Blue at a deflection of 0.5 mm, i.e. within the elastic range, was the smallest at 0.32 N. The loads for WaveOne Gold, ProTaper Next, ProTaper Gold, and WaveOne increased gradually to 0.41, 0.52, 0.53, and 0.77 N, respectively. The load for ProTaper was 1.42 N, which was significantly higher than for the former five samples with the exception of WaveOne (*P* < 0.05). In addition, the loads for Reciprocal Blue and WaveOne Gold were 2.09 and 2.34 N at a deflection of 3.0 mm, i.e. within the superelastic range, being significantly lower than that of ProTaper (4.23 N) and WaveOne (4.39 N) (*P* < 0.05). Furthermore,

the loads for ProTaper Gold (3.12 N) and ProTaper Next (3.10 N) were not significantly different.

Cyclic fatigue

NCFs and lengths of the fractured segments of the six files investigated are listed in Table 5. NCF data for all six files and fragment lengths for WaveOne Gold and ProTaper Gold were normally distributed. NCF data showed no homoscedasticity (*P* < 0.001). NCFs differed significantly among the six files (*P* < 0.001) while the lengths of the fractured segments showed no significant differences (*P* = 0.109). WaveOne Gold generated the largest statistically significant NCF of 560 \pm 111, implying the highest significant fatigue resistance. The NCF for ProTaper (65 \pm 20) was the lowest and the fatigue resistance was considered as the lowest. The mean NCFs for Reciprocal Blue and ProTaper Next were 153 and 158, respectively. The mean NCF for ProTaper Gold (222) was significantly higher than that for WaveOne (128, *P* < 0.05). The differences among ProTaper Gold, ProTaper Next and WaveOne were shown to be non-significant statistically. The mean lengths of the fractured segments of the six files were approximately 6.9 mm, demonstrating no significant differences within the group. Finally, the topographic appearance of the fractured surfaces of all instruments presented typical features of cyclic fatigue, including crack initiation areas, the presence of fatigue striations and a fast fracture zone with dimples. In particular, two crack initiation areas were observed in the gold and blue instruments (Fig. 4).

Table 5 NCF and fragment length for the six files studied

		WaveOne Gold	ProTaper Gold	Reciproc Blue	ProTaper Next	WaveOne	ProTaper	H	P
NCF	Mean \pm SD	560 \pm 111 ^{cd}	222 \pm 36 ^{ef}	153 \pm 41 ^a	158 \pm 22 ^{af}	128 \pm 18 ^{ab}	65 \pm 20 ^{abd}	50.286	<0.001
	P_{K-S}	0.2	0.134	0.2	0.2	0.067	0.063		
Fragment length (mm)	Mean \pm SD	6.83 \pm 0.41	6.84 \pm 0.21	6.82 \pm 0.19	6.92 \pm 0.10	7.01 \pm 0.03	6.93 \pm 0.17	9.007	0.109
	Median (IQR)		6.90 (0.19)		6.99 (0.19)	7.00 (0.01)	6.99 (0.08)		

All data are generally presented as mean \pm standard deviation (SD). The normality of data was analyzed using the Kolmogorov-Smirnov test. Abnormally distributed data are also presented as median (IQR). The homogeneity of variables was analyzed using the Levene test. Comparisons among groups were performed using the Kruskal-Wallis H test with Bonferroni *post hoc* test. $n = 10$ in each group. ^aCompared with WaveOne Gold ($P < 0.05$). ^bCompared with ProTaper Gold ($P < 0.055$). ^cCompared with Reciproc Blue ($P < 0.055$). ^dCompared with ProTaper Next ($P < 0.05$). ^eCompared with WaveOne ($P < 0.05$). ^fCompared with ProTaper ($P < 0.05$)

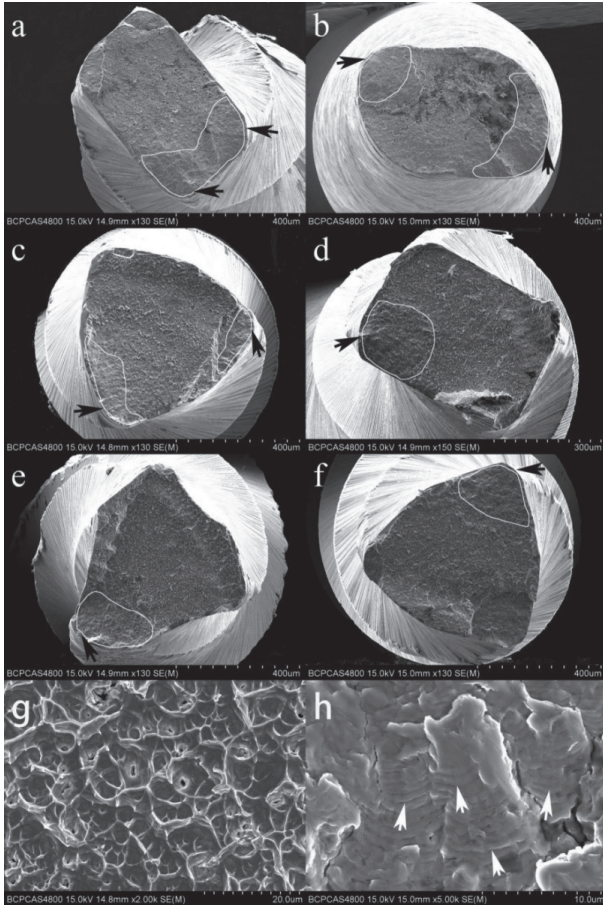


Fig. 4 Topographic features of the six files (a) WaveOne Gold, (b) Reciproc Blue, (c) ProTaper Gold, (d) ProTaper Next, (e) WaveOne, (f) ProTaper. Crack origins (white circles) and fatigue crack propagation and dimple areas (g) are identified in (a)–(f); black arrows indicate the crack initiation origin; white arrows indicate the fatigue striations in (h). Figs. (g) and (h) are from ProTaper and Reciproc Blue samples, respectively.

Discussion

The mechanical properties of NiTi alloys are determined by their phase transformation behaviors, which in turn are governed by their chemical compositions and thermomechanical procedures combining mechanical deformation and heat treatment. Previous reports have shown that not only transformation characteristics but also mechanical properties, notably the superelastic properties of NiTi files, are altered by their thermomechanical history [23]. In addition, the mechanical properties of NiTi files can be greatly altered through variations in instrument configuration. In other words, despite the enhancement of file flexibility by specific thermal manipulations, the actual results may vary.

More recently, gold and blue heating processes have been used to fabricate NiTi files to achieve different crystalline phase structures that improve flexibility and fatigue resistance. The newly produced WaveOne Gold, ProTaper Gold and Reciproc Blue have also been widely used. However, the phase transformation behaviors of these new NiTi instruments and the relationships with their mechanical properties have remained unclear.

Thermomechanical treatment of NiTi alloys has a strong impact on their

transformation behavior. Martensitic transformation of near-equiatomic NiTi alloys occurs in a single-stage procedure (austenite [A]-martensite [M]) or a two-stage one (A-R-M), depending on their thermomechanical history [24]. Generally, Ni-rich NiTi alloys undergo a single-stage transformation [24]. Special heat treatment can lead to the appearance of finely dispersed Ti_3Ni_4 precipitates in the austenitic matrix and a switch to two-stage transformation [24]. Such Ti_3Ni_4 precipitates limit the formation of martensite during the cooling step, along with the deformation of a large lattice. However, the formation of R-phase coinciding with the deformation of a much smaller lattice is not affected by Ti_3Ni_4 precipitates. The R-phase, considered to be another potential martensite phase, shows a preference for the presence of fine particles rather than martensite. Therefore, further cooling steps are required for formation of martensite and the two-stage martensitic transformation.

DSC analysis is a common method for examining the phase transformation behaviors of NiTi files [6,22]. The DSC results in the present work show that the A_f temperatures of the WaveOne Gold and ProTaper Gold instruments were higher than 50°C. The presence of martensite variants can be related to high transformation temperatures [7]. Their enthalpy variations (ΔH) during heating and cooling were larger than those of ProTaper Next, WaveOne and ProTaper, suggesting that WaveOne Gold and ProTaper Gold had martensite structures at body temperature. In contrast, ProTaper Next and WaveOne, both made from M-wires, have a large amount of work-hardened martensitic structures and superelastic properties, although their A_f temperatures also are higher than 50°C. The A_f temperature of Reciproc Blue was $38.4 \pm 0.6^\circ C$, i.e. close to body temperature. Coincidentally, another blue file, Vortex Blue, demonstrated the highest enthalpy variations (ΔH) during heating and cooling, suggesting that many more grains were involved in the phase transformation behavior [23]. Therefore, it can be suggested that the transformation temperature can be altered in different heat treatment processing steps through the release of crystal lattice defects and elimination of internal strain energy.

Two overlapping endothermic peaks were observed in the heating curves of WaveOne Gold, ProTaper Gold and Reciproc Blue, suggesting the generation of an intermediate R-phase during phase transformation [19]. The first peak during the heating stage is related to the phase transformation from martensite to R-phase. The second peak, at the higher temperature, is assigned to the subsequent phase transformation from R-phase to austenite. Thus, the thermomechanical processing procedure created Ti_3Ni_4 precipitates that are believed to exist during such two-stage transformations. During cooling, exothermal peaks were also noted for WaveOne Gold, ProTaper Gold and Reciproc Blue, which are related to the phase transformation from austenite to R-phase. The subsequent transformations of R-phase to martensite, however, were difficult to detect except in Reciproc Blue. It has been reported that Vortex Blue presented an A-R-M phase transformation during heating and cooling, and only a single peak indicative of single-phase transformation was found for ProFile Vortex made from M-wire during these processes [25]. It has also been mentioned that the A_f temperature of Vortex Blue (38°C) was lower than that of ProFile Vortex (50°C) [25,26]. Hieawy et al. further reported that ProTaper Gold achieved a two-stage specific transformation behavior and high A_f temperatures [7]. A two-stage phase transformation during heating and single-stage phase transformation during cooling were observed for ProTaper, resulting in complete austenite structures at body temperature (37°C), consistent with a previous study [27].

Bending properties and cyclic fatigue resistance are considered among the most important mechanical properties of NiTi rotary instruments, providing fundamental information for the correct choice of suitable

medical equipment. When the ambient temperature is higher than the Af temperature, superelasticity or pseudo-elasticity occurs with the phase transformation of NiTi alloys during the application of stress exceeding a critical level. For this reason, conventional superelastic NiTi instruments require the working temperature to be higher than the Af to achieve pseudo-elasticity. The Af temperatures for ProFile and ProTaper, which exhibit superelasticity during clinical application, are lower than body temperature [28,29]. The present bending load curves suggested that WaveOne Gold and ProTaper Gold also exhibited superelasticity, despite having a working temperature below the Af. The DSC results showed that gold instruments had 2-stage specific transformation behavior, indicating that reverse transformation of the alloy occurred via the intermediate R-phase, thereby reflecting the complex phase transformation associated with the manufacturing process. However, Reciproc Blue did not present an evident rebound effect after unloading, similar to the CM wire. Their behavior may be explained by the presence of stable martensite [28]. Interestingly, the metallurgical characteristics of Reciproc Blue files exhibited 2-stage specific transformation behavior but lower Af temperatures, contrary to the CM Wire. Therefore, it is suggested that gold heat treatment can preserve the superelastic property of NiTi instruments. Blue heat treatment, however, can create shape memory properties, i.e. hysteresis superelasticity.

The bending load values of WaveOne Gold and ProTaper Gold in the superelastic range were higher than that of Reciproc Blue instruments but lower than those of the other three studied. It has been reported that the shear modulus in the R-phase of gold and blue instruments is smaller than that of martensite and austenite [30]. In addition, the transformation strain for R-phase transformation less than one tenth of that seen in martensitic transformation [31]. The bending load within the superelastic range depends upon the critical stress required to trigger martensitic phase transformation; at a low Ms temperatures the phase transformation is limited and more stress is needed to trigger it [26]. Therefore, critical stress is increased by reducing the Ms temperature. Here, the Ms temperatures of WaveOne Gold and ProTaper Gold were higher than that of ProTaper, resulting in low load values in the superelastic range. However, Reciproc Blue presented a unique result. On one hand, even though the Ms temperature of Reciproc Blue was lower than those of WaveOne Gold and ProTaper Gold, its bending load was also lower possibly due to the unique blue heat treatment. On the other hand, Reciproc Blue had the smallest cross-sectional area and inner core area (Table 4). Although the Ms temperatures of WaveOne Gold, ProTaper Gold, WaveOne and ProTaper were close to each other, their bending loads were significantly different. A large amount of work was needed to harden martensite in M-wire, with a higher shear modulus than that of unloaded martensite and austenite, leading to different phase compositions at body temperature. The details of thermomechanical treatment for gold and blue files remain unknown. However, the present results demonstrate that the mechanical behaviors are closely related to the phase transformation temperatures determined by thermomechanical history and instrument configurations.

Both gold and blue heat treatment NiTi files show improved fatigue resistance when compared with M-Wire and conventional superelastic wire (Table 5). Heat treatment files have different fatigue resistances due to the existence of martensite variants that are related to the high phase transformation temperatures of gold and blue files. Figueiredo et al. reported that the NCF of martensitic NiTi wires can be at least 100 times higher than for superelastic and stable austenitic NiTi alloys [32]. Here, gold and blue files were more flexible than the other files. For a given strain, a file with increased flexibility would experience less stress, allowing for a longer fatigue lifetime given that all other factors (cross section, design, etc.) remain the same. Thus, gold and blue files go through less stress and have a longer fatigue lifetime. Furthermore, the required number of loading cycles needed to initiate a fatigue crack and to facilitate crack propagation to a critical size is considered to represent the fatigue life of NiTi files. The mechanism of crack propagation in martensite shows that a large number of highly branched cracks slowly propagate. However, only a few fatigue cracks nucleate in superelastic NiTi, resulting in faster propagation [33]. A previous study found that CM Wire NiTi files had multiple crack origins on the fracture surface [34]. Similarly, in the present study, thermally treated gold and blue instruments exhibited superior cyclic fatigue resistance compared with other instruments and the fractographic features showed initiation of more than one crack area.

As reported previously, two of the reciprocating files investigated here, WaveOne Gold and Reciproc Blue, have excellent cyclic fatigue resistance [17,35]. In comparison with rotary motion, the cyclic fatigue resistance of NiTi files can be increased by the reciprocation motion [36]. Gold heat treatment used to produce WaveOne Gold files increases the flexibility of the files. The molecular structures of Reciproc Blues files are altered by the new heat treatment during production. As mentioned before, the bending load of Reciproc blue was smaller than that of WaveOne Gold (Table 4). Thus, the cyclic fatigue of Reciproc blue is theoretically more resistant than that of WaveOne Gold. However, as studied, the cyclic fatigue resistance of WaveOne Gold is higher than that of Reciproc Blue. Therefore, gold heat treatment can result in better cyclic fatigue resistance than blue heat treatment. This result, however, is contrary to previous studies [37,38], possibly due to the variance in experimental cyclic fatigue devices. For example, the files in the Silva et al. study were tested in severely curved canals [38]. In addition to the reciprocation motion, the better cyclic fatigue could have been attributable to the cross-sectional parallelogram shape and off-center design of the WaveOne Gold instrument.

Files made from M-wire have been reported to have higher cyclic fatigue resistance than those made of conventional NiTi alloys [39]. In the present study, similar results confirmed that the NCFs of WaveOne and ProTaper Next were higher than that of ProTaper, which is believed to be composed of conventional NiTi alloys. Due to its own features, such as cross-section, speed, and rotary approaches, the NCF of ProTaper Next exceeded that of WaveOne.

In summary, after gold heat treatment and blue heat treatment, NiTi instruments presented significantly better bending properties and cyclic fatigue resistances, in comparison with M-wire and conventional instruments, demonstrating their improved performance. Gold heat treatment can preserve the superelastic properties of NiTi instruments, while shape memory properties, i.e. hysteresis superelasticity, are created by blue heat treatment. In addition, gold heat treatment resulted in better cyclic fatigue resistances than blue heat treatment.

Acknowledgments

This work was supported by two funds: The National Natural Science Foundation of China (81200826) and the National Key Research and Development Program of China (2016YFB1101200).

Conflict of interest

The authors declare that they have no conflict of interest.

References

- Peters OA (2004) Current challenges and concepts in the preparation of root canal systems: a review. *J Endod* 30, 559-567.
- Plotino G, Testarelli L, Al-Sudani D, Pongione G, Grande NM, Gambarini G (2014) Fatigue resistance of rotary instruments manufactured using different nickel-titanium alloys: a comparative study. *Odontology* 102, 31-35.
- Walia HM, Brantley WA, Gerstein H (1988) An initial investigation of the bending and torsional properties of Nitinol root canal files. *J Endod* 14, 346-351.
- Ninan E, Berzins DW (2013) Torsion and bending properties of shape memory and superelastic nickel-titanium rotary instruments. *J Endod* 39, 101-104.
- Peters OA, Peters CI, Schonenberger K, Barbakow F (2003) ProTaper rotary root canal preparation: effects of canal anatomy on final shape analysed by micro CT. *Int Endod J* 36, 86-92.
- Shen Y, Zhou HM, Wang Z, Campbell L, Zheng YF, Haapasalo M (2013) Phase transformation behavior and mechanical properties of thermomechanically treated K3XF nickel-titanium instruments. *J Endod* 39, 919-923.
- Hieawy A, Haapasalo M, Zhou H, Wang ZJ, Shen Y (2015) Phase transformation behavior and resistance to bending and cyclic fatigue of protaper gold and protaper universal instruments. *J Endod* 41, 1134-1138.
- Alapati SB, Brantley WA, Svec TA, Powers JM, Nusstein JM, Daehn GS (2005) SEM observations of nickel-titanium rotary endodontic instruments that fractured during clinical use. *J Endod* 31, 40-43.
- Iqbal MK, Kohli MR, Kim JS (2006) A retrospective clinical study of incidence of root canal instrument separation in an endodontics graduate program: a PennEndo database study. *J Endod* 32, 1048-1052.
- Johnson E, Lloyd A, Kuttler S, Namerow K (2008) Comparison between a novel nickel-titanium alloy and 508 nitinol on the cyclic fatigue life of ProFile 25/.04 rotary instruments. *J Endod* 34, 1406-1409.
- Gambarini G, Gerosa R, De Luca M, Garala M, Testarelli L (2008) Mechanical properties of a new and improved nickel-titanium alloy for endodontic use: an evaluation of file flexibility. *Oral Surg Oral Med Oral Pathol Oral Radiol Endod* 105, 798-800.
- Larsen CM, Watanabe I, Glickman GN, He J (2009) Cyclic fatigue analysis of a new generation of nickel titanium rotary instruments. *J Endod* 35, 401-403.
- Testarelli L, Plotino G, Al-Sudani D, Vincenzi V, Giansiracusa A, Grande NM et al. (2011) Bending properties of a new nickel-titanium alloy with a lower percent by weight of nickel.

- J Endod 37, 1293-1295.
14. Gao Y, Gutmann JL, Wilkinson K, Maxwell R, Ammon D (2012) Evaluation of the impact of raw materials on the fatigue and mechanical properties of ProFile Vortex rotary instruments. *J Endod* 38, 398-401.
 15. Shen Y, Zhou HM, Zheng YF, Peng B, Haapasalo M (2013) Current challenges and concepts of the thermomechanical treatment of nickel-titanium instruments. *J Endod* 39, 163-172.
 16. Haapasalo M, Shen Y (2013) Evolution of nickel-titanium instruments: from past to future. *Endod Topics* 29, 3-17.
 17. Ozyurek T (2016) Cyclic fatigue resistance of reciproc, waveone, and waveone gold nickel-titanium instruments. *J Endod* 42, 1536-1539.
 18. Uygun AD, Kol E, Topcu MK, Seckin F, Ersoy I, Tanriver M (2016) Variations in cyclic fatigue resistance among ProTaper Gold, ProTaper Next and ProTaper Universal instruments at different levels. *Int Endod J* 49, 494-499.
 19. Keskin C, Inan U, Demiral M, Keles A (2017) Cyclic fatigue resistance of reciproc blue, reciproc, and waveone gold reciprocating instruments. *J Endod* 43, 1360-1363.
 20. De-Deus G, Silva EJ, Vieira VT, Belladonna FG, Elias CN, Plotino G et al. (2017) Blue thermomechanical treatment optimizes fatigue resistance and flexibility of the reciproc files. *J Endod* 43, 462-466.
 21. Silva E, Hecksher F, Antunes HDS, De-Deus G, Elias CN, Vieira VTL (2018) Torsional fatigue resistance of blue-treated reciprocating instruments. *J Endod* 44, 1038-1041.
 22. Hou X, Yahata Y, Hayashi Y, Ebihara A, Hanawa T, Suda H (2011) Phase transformation behaviour and bending property of twisted nickel-titanium endodontic instruments. *Int Endod J* 44, 253-258.
 23. Frick CP, Ortega AM, Tyber J, Gall K, Maier HJ, Liu Y (2005) Thermal processing of polycrystalline niti shape memory alloys. *Materials Science & Engineering A* 405, 34-49.
 24. Otsuka K, Ren X (2005) Physical metallurgy of Ti-Ni-based shape memory alloys. *Prog Mater Sci* 50, 511-678.
 25. Shen Y, Zhou H, Coil JM, Aljazaeri B, Buttar R, Wang Z et al. (2015) Profile vortex and vortex blue nickel-titanium rotary instruments after clinical use. *J Endod* 41, 937-942.
 26. Tsujimoto M, Irifune Y, Tsujimoto Y, Yamada S, Watanabe I, Hayashi Y (2014) Comparison of conventional and new-generation nickel-titanium files in regard to their physical properties. *J Endod* 40, 1824-1829.
 27. Zhou HM, Shen Y, Zheng W, Li L, Zheng YF, Haapasalo M (2012) Mechanical properties of controlled memory and superelastic nickel-titanium wires used in the manufacture of rotary endodontic instruments. *J Endod* 38, 1535-1540.
 28. Miyai K, Ebihara A, Hayashi Y, Doi H, Suda H, Yoneyama T (2006) Influence of phase transformation on the torsional and bending properties of nickel-titanium rotary endodontic instruments. *Int Endod J* 39, 119-126.
 29. Shen Y, Zhou HM, Zheng YF, Campbell L, Peng B, Haapasalo M (2011) Metallurgical characterization of controlled memory wire nickel-titanium rotary instruments. *J Endod* 37, 1566-1571.
 30. Thomasová M, Sedlák P, Seiner H, Janovská M, Kabla M, Shilo D et al. (2015) Young's moduli of sputter-deposited NiTi films determined by resonant ultrasound spectroscopy: austenite, r-phase, and martensite. *Scr Mater* 101, 24-27.
 31. Wu SK, Lin HC, Chou TS (1990) A study of electrical resistivity, internal friction and shear modulus on an aged Ti 49 Ni 51 alloy. *Acta Metallurgica Et Materialia* 38, 95-102.
 32. Figueiredo AM, Modenesi P, Buono V (2009) Low-cycle fatigue life of superelastic NiTi wires. *Int J Fatigue* 31, 751-758.
 33. Mckelvey AL, Ritchie RO (2001) Fatigue-crack growth behavior in the superelastic and shape-memory alloy nitinol. *Metallurgical & Materials Transactions A* 32, 731-743.
 34. Shen Y, Qian W, Abtin H, Gao Y, Haapasalo M (2011) Fatigue testing of controlled memory wire nickel-titanium rotary instruments. *J Endod* 37, 997-1001.
 35. Topcuoglu HS, Duzgun S, Akti A, Topcuoglu G (2017) Laboratory comparison of cyclic fatigue resistance of WaveOne Gold, Reciproc and WaveOne files in canals with a double curvature. *Int Endod J* 50, 713-717.
 36. Karatas E, Arslan H, Buker M, Seckin F, Capar ID (2016) Effect of movement kinematics on the cyclic fatigue resistance of nickel-titanium instruments. *Int Endod J* 49, 361-364.
 37. Gundogar M, Ozyurek T (2017) Cyclic fatigue resistance of oneshape, hyflex edm, waveone gold, and reciproc blue nickel-titanium instruments. *J Endod* 43, 1192-1196.
 38. Silva E, Vieira VTL, Hecksher F, Dos Santos Oliveira MRS, Dos Santos Antunes H, Moreira EJM (2018) Cyclic fatigue using severely curved canals and torsional resistance of thermally treated reciprocating instruments. *Clin Oral Investig* 22, 2633-2638.
 39. Varghese NO, Pillai R, Sujathen UN, Sainudeen S, Antony A, Paul S (2016) Resistance to torsional failure and cyclic fatigue resistance of ProTaper Next, WaveOne, and Mtwo files in continuous and reciprocating motion: an in vitro study. *J Conserv Dent* 19, 225-230.